IMPACT-INDUCED SEISMIC PROPERTIES FOR A RANGE OF MARTIAN TOP CRUST ANALOGUES CALCULATED FROM NUMERICAL IMPACT MODELLING. A. Rajšić[1], K. Miljković[1], N. Wójcicka[2], G. S. Collins[2], A. Lagain[1], I. J. Daubar[3]. [2]Space Science and Technology Centre, School of Earth and Planetary Sciences, Curtin University, Perth, Australia; [2]Department of Earth Science and Engineering, Imperial College London, London, SW7 2AZ, United Kingdom; [3]Brown University, Providence, Rhode Island, US; (E-mail: andrea.rajsic@postgrad.curtin.edu.au).

Introduction: Since landing on Mars in late 2018 [1], several hundred seismic events have been recorded by NASA's InSight seismometer [2]. However, identifying impact events in the seismic data has proven challenging [3]. Numerical impact modelling contributes to the understanding of impact event seismic detectability. Previous numerical modelling work that considered impacts in uniform targets [4, 5] showed that target properties can influence the efficiency of conversion of impact energy to seismic energy and seismic source magnitude (seismic moment). In this work, more realistic target analogues for small impacts on Mars were employed.

The aim is to: 1) Estimate the regolith thickness at the location of an impact known to have occurred within the InSight mission timeframe, based on rocky ejecta crater mapping as input to a two-layer near-surface structure; 2) Define a relationship between impact momentum and seismic moment, and a relationship between seismic moment and seismic energy, valid for a range of martian upper crust analogues.

Crater mapping and regolith thickness estimate: Rocky ejecta craters (REC) craters have identifiable boulders in the ejecta surrounding a crater, which were likely excavated from the underlying bedrock during impact (Fig. 1). REC observations can be used to estimate the overlaying regolith thickness [e.g., 6, 7, and refs therein]. This method showed that the top regolith layer is between 3-17 m in thickness proximal to the InSight lander [7, 8]. We mapped REC craters 700 km away from the InSight lander at 6.5°N, 148°E (HiRISE image $ESP0473761865$), in the vicinity of a new impact that was confirmed in orbital imagery to have occured between 13/08/2019 and 1/09/2020, during the time InSight has been observing [9].

We mapped 1155 simple craters and classified them as rocky ejecta (RECs) and non-rocky ejecta (nRECs). Diameters of mapped craters were used to estimate the local regolith thickness. RECs were used to estimate maximum regolith thickness, and nRECs minimum [7]. The smallest crater had a diameter of 2 m and the largest 103 m. The median diameter was 10 m. Most of the measured craters are between 5 and 15 m in diameter. Of these, only 1.4% (16 craters total) were RECs. The smallest and largest REC craters were 15.3 m and 103 m in diameter, respectively. The smallest and largest nREC craters were 2 m and 48 m in diameter, respectively.

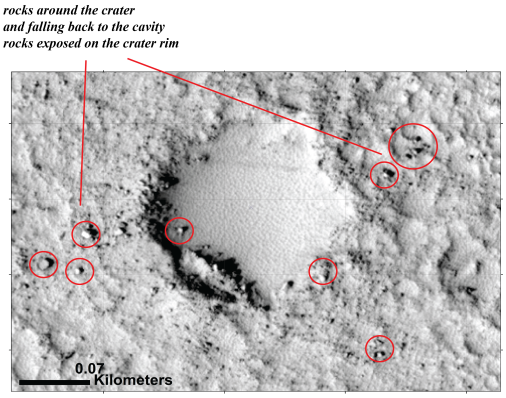

Figure 1: Example of a rocky ejecta crater (REC) with marked boulders used as criteria for identification.

An average estimate of regolith thickness was made with the approach of [10], where the excavation depth was considered to be 0.084 times the crater diameter. In this case, the regolith thickness is estimated to be between 4 m to 8.62 m. Our mapping area is in the late Amazonian volcanic unit [e.g., 11], while InSight landing site (3-17 m regolith thickness [e.g., 7]) is in early Hesperian transition unit. This result suggests that the younger geological units may have a thinner regolith layer, most likely due to shorter exposure to impact gardening, one of the main process involved in regolith production. We combine our estimate (since InSight is surrounded by these units) with the estimate of [7] and vary regolith thickness between 5 and 15 m in our numerical models in order to be applicable to a wide variety of targets in the InSight region.

Numerical impact modelling: Numerical impact simulations were made using the iSALE-2D shock physics code (https://isale-code.github.io/). Impact momentum was varied between 7x10^2 kgms^{-1} and 9.08x10^6 kgms^{-1} in order to simulate pressure wave propagation for impacts that would form craters between 1.5 and 26 m in diameter. This is the expected crater diameter range to occur on Mars during lifetime of the InSight mission [e.g., 3]. Impact conditions applied here are described in detail in [4, 5].

We investigated impact scenarios in: a) a single-layer bedrock and fractured bedrock targets (25% porosity) and b) layered targets appropriate for REC morphology, where the thickness of the upper regolith layer was 5, 10, or

15 m. Beneath the regolith layer was either non-porous bedrock or fractured, sandstone-like 25% porous bedrock. Material models for all layers and appropriate impact conditions for small impacts on Mars have previously been explained in [4, 5]. The speed of sound in the target was calculated as the speed of the pressure wave between two pre-selected cells (gauges). The seismic efficiency and seismic moment were calculated as shown in our previous works [4, 5, 12].

The relationship between the seismic moment, M, and impact momentum, p_i, in different target materials is shown in Fig. 2. The data shown in Fig. 2 is from all simulations. Results show that there is a modest decrease in seismic moment when a regolith layer is introduced. This is in agreement with Eq. 20 from [4] and shows that the seismic moment calculated from simulations is of the same order of magnitude for different target properties. Seismic moment is proportional to the impact momentum which is in agreement with observations on the Moon [e.g., 13, 14].

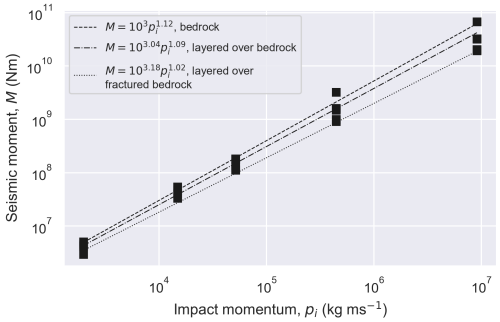

Figure 2: The seismic moment, M, as a function of impact momentum, p_i, in all scenarios. The square points denote calculations from individual numerical simulations. Seismic moment in fractured bedrock follows the same function as in layered targets overlying bedrock (dash dotted line), bedrock is shown in dashed line and layered targets over fractured bedrock in dotted line.

Fig. 3 shows the relationship between the seismic moment and seismic energy. The seismic energy (E_s) is calculated from seismic efficiency, k ($k = \frac{E_s}{E_k}$, where E_k is impact kinetic energy). The seismic energy produced by impacts in layered targets is marked by triangles in Fig. 3. They are compared to the scaling relationships derived in [4] for regolith-only targets. The largest difference is for the uniform bedrock target, where seismic energy was up to three orders higher than in case of regolith-only and layered targets, for the same impact conditions, while layered targets are very similar to the regolith-only targets.

Conclusions: Crater mapping and regolith thickness estimates (4-9 m) inform realistic models of the near-surface of Mars for modelling impact-generated seismic waves. The resulting seismic moment for small impacts on Mars varies by only a factor of four across different targets from strong bedrock to thick, weak porous regolith. For all target structures, as seismic moment increases the seismic energy deposited in the target increases (Fig. 3). In layered targets, the seismic energy of small impacts is comparable to that for regolith-only targets, but for larger impacts, the seismic energy estimate is higher than in regolith-only targets and appears to converge towards the bedrock-only scenario. This is because small impacts tend to excavate/deposit more kinetic energy within the top layer (here assumed as regolith) and larger impacts excavate into the bedrock underneath. These newly constrained relationships could be used in application to newly formed impacts, in order to estimate their detectability in seismic data.

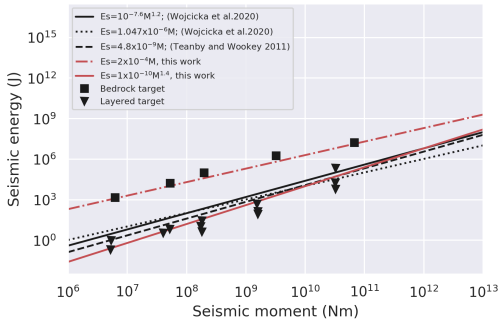

Figure 3: Seismic energy as a function of the seismic moment, in bedrock and all layered targets (bedrock is 0% porous). Red lines are from this work, and black lines are from [4] and [15]. Triangles are individual simulations made into layered targets and square denote impact simulation results made into bedrock.

Acknowledgements: We gratefully acknowledge the developers of iSALE (www.isale-code.de). AR and KM are fully funded by the Australian Research Council (DE180100584, DP180100661). NW and GSC are funded by the UK Space Agency (ST/S001514/1, ST/T002026/1).

References: [1] Banerdt, W. B. et al. (2020) *Nature geo.*1–7. [2] Clinton, J. & Euchner, F. (2021). [3] Daubar, I. et al. (2018) *SSR*, 214:1–68. [4] Wojcicka, N. et al. (2020) *JGR:Planets*, 125. [5] Rajšić, A et al. (2021b) *JGR:Planets*, [6] Wilcox, B. et al. (2005) *MAPS*, 40:695–710. [7] Warner, N. et al. (2017) *SSR*, 211:147–190. [8] Golombek, M et al. (2020) *Nature comms.* 11:1–11. [9] Miljkovic, K. et al. (2021) *52nd LPSC* Houston: LPI, Abstract #1758. [10] Melosh, H. J. (1989) *icgp*, [11] Tanaka, K. et al. (2014). [12] Rajšić, A et al. (2021a) *ESS*, [13] Lognonné, P. et al. (2009) *JGR:Planets*, 114. [14] Gudkova, T. et al. (2015) *EPSL*, 427:57–65. [15] Teanby, N. & Wookey, J (2011) *Phys. Earth Planet. Inter.* 186:70–80.